

## Expansion of the tetragonal magnetic phase with pressure in the iron arsenide superconductor $\text{Ba}_{1-x}\text{K}_x\text{Fe}_2\text{As}_2$

E. Hassinger,<sup>1,\*</sup> G. Gredat,<sup>1</sup> F. Valade,<sup>1</sup> S. René de Cotret,<sup>1</sup> O. Cyr-Choinière,<sup>1</sup> A. Juneau-Fecteau,<sup>1</sup> J.-Ph. Reid,<sup>1</sup> H. Kim,<sup>2</sup> M. A. Tanatar,<sup>2</sup> R. Prozorov,<sup>2,3</sup> B. Shen,<sup>4</sup> H.-H. Wen,<sup>4,5</sup> N. Doiron-Leyraud,<sup>1</sup> and Louis Taillefer<sup>1,5,†</sup>

<sup>1</sup>*Département de Physique & RQMP, Université de Sherbrooke, Sherbrooke, Québec J1K 2R1, Canada*

<sup>2</sup>*Ames Laboratory, Ames, Iowa 50011, USA*

<sup>3</sup>*Department of Physics and Astronomy, Iowa State University, Ames, Iowa 50011, USA*

<sup>4</sup>*Center for Superconducting Physics and Materials, National Laboratory of Solid State Microstructures and Department of Physics, Nanjing University, Nanjing 210093, China*

<sup>5</sup>*Canadian Institute for Advanced Research, Toronto, Ontario M5G 1Z8, Canada*

(Received 17 December 2015; revised manuscript received 2 March 2016; published 1 April 2016)

In the temperature-concentration phase diagram of most iron-based superconductors, antiferromagnetic order is gradually suppressed to zero at a critical point, and a dome of superconductivity forms around that point. The nature of the magnetic phase and its fluctuations is of fundamental importance for elucidating the pairing mechanism. In  $\text{Ba}_{1-x}\text{K}_x\text{Fe}_2\text{As}_2$  and  $\text{Ba}_{1-x}\text{Na}_x\text{Fe}_2\text{As}_2$ , it has recently become clear that the usual stripelike magnetic phase, of orthorhombic symmetry, gives way to a second magnetic phase, of tetragonal symmetry, near the critical point, in the range from  $x = 0.24$  to  $x = 0.28$  for  $\text{Ba}_{1-x}\text{K}_x\text{Fe}_2\text{As}_2$ . In a prior study, an unidentified phase was discovered for  $x < 0.24$  but under applied pressure, whose onset was detected as a sharp anomaly in the resistivity. Here we report measurements of the electrical resistivity of  $\text{Ba}_{1-x}\text{K}_x\text{Fe}_2\text{As}_2$  under applied hydrostatic pressures up to 2.75 GPa, for  $x = 0.22, 0.24$ , and  $0.28$ . The critical pressure above which the unidentified phase appears is seen to decrease with increasing  $x$  and vanish at  $x = 0.24$ , thereby linking the pressure-induced phase to the tetragonal magnetic phase observed at ambient pressure. In the temperature-concentration phase diagram of  $\text{Ba}_{1-x}\text{K}_x\text{Fe}_2\text{As}_2$ , we find that pressure greatly expands the tetragonal magnetic phase, while the stripelike phase shrinks. This reveals that pressure may be a powerful tuning parameter with which to explore the interplay between magnetism and superconductivity in this material.

DOI: [10.1103/PhysRevB.93.144401](https://doi.org/10.1103/PhysRevB.93.144401)

### I. INTRODUCTION

The phase diagram of iron-based superconductors of the  $\text{BaFe}_2\text{As}_2$  family is characterized by competing antiferromagnetic (AF) order and superconductivity. Usually, the AF order decreases with concentration (doping) and a dome of superconductivity surrounds the critical point [1]. The AF order is a stripelike spin-density wave, with a wave vector  $\mathbf{Q} = (\pi, 0)$  and the magnetic moments lying in the plane. At the magnetic transition temperature, or slightly above it, the lattice changes from tetragonal at high temperature to orthorhombic at low temperature [2,3].

In  $\text{Ba}_{1-x}X_x\text{Fe}_2\text{As}_2$ , where  $X = \text{K}$  or  $\text{Na}$ , the phase diagram was recently found to be richer than this simple picture. Resistivity measurements under pressure revealed the existence of an internal transition inside the AF phase of  $\text{Ba}_{1-x}\text{K}_x\text{Fe}_2\text{As}_2$  [4]. As the onset temperature  $T_N$  of the orthorhombic AF phase (o-AF) is suppressed with hydrostatic pressure  $P$ , an additional phase transition to a “new phase” appears below a transition temperature  $T_0 < T_N$ , for  $0.16 < x < 0.21$ , when  $P > 0.9$  GPa [4]. A tetragonal magnetic phase (t-AF) was then discovered in the closely related compound  $\text{Ba}_{1-x}\text{Na}_x\text{Fe}_2\text{As}_2$ , by neutron and x-ray diffraction on powder samples [5]. Subsequent neutron scattering on single crystals showed that in this t-AF phase the spins are aligned parallel to the  $c$  axis [6]. A similar phase of tetragonal symmetry was then found in

$\text{Ba}_{1-x}\text{K}_x\text{Fe}_2\text{As}_2$  at ambient pressure, for  $0.24 < x < 0.28$  [7]. The magnetic moments in the t-AF phase of  $\text{Ba}_{1-x}\text{K}_x\text{Fe}_2\text{As}_2$  are also oriented along the  $c$  axis [8,9]. Infrared spectroscopy showed that the t-AF phase has a double- $Q$  magnetic structure [8], as opposed to the single- $Q$  structure of the o-AF phase. A pressure study of a  $\text{Ba}_{1-x}\text{K}_x\text{Fe}_2\text{As}_2$  sample with  $x = 0.15$  by specific heat, transport, and the Nernst effect confirms the bulk nature of the sequence of phase transitions previously detected only in resistivity [10]. Additionally, the authors show that the pressure-induced “new phase” suppresses the large Nernst signal of the o-AF phase, indicating the suppression of the nematicity as in the t-AF phase at ambient pressure. Several theoretical studies have investigated the properties of the tetragonal magnetic phase in iron-based superconductors [5,11–20].

In this article, we extend our prior study of  $\text{Ba}_{1-x}\text{K}_x\text{Fe}_2\text{As}_2$  under pressure, performed up to  $x = 0.21$  [4], by studying three further samples, with  $x = 0.22, 0.24$ , and  $0.28$ . We are able to connect the additional phase induced by pressure with the tetragonal phase seen at ambient pressure. Pressure is seen to cause a dramatic expansion of the tetragonal magnetic phase, on the backdrop of a shrinking orthorhombic phase.

### II. METHODS

Single crystals of  $\text{Ba}_{1-x}\text{K}_x\text{Fe}_2\text{As}_2$  were grown from self-flux [21]. Three underdoped samples were measured, with a superconducting transition temperature  $T_c = 20.8 \pm 0.5, 25.4 \pm 0.5$ , and  $30.1 \pm 0.5$  K, respectively. Using the relation between  $T_c$  and the nominal K concentration  $x$  reported in

\*elena.hassinger@usherbrooke.ca

†louis.taillefer@usherbrooke.ca

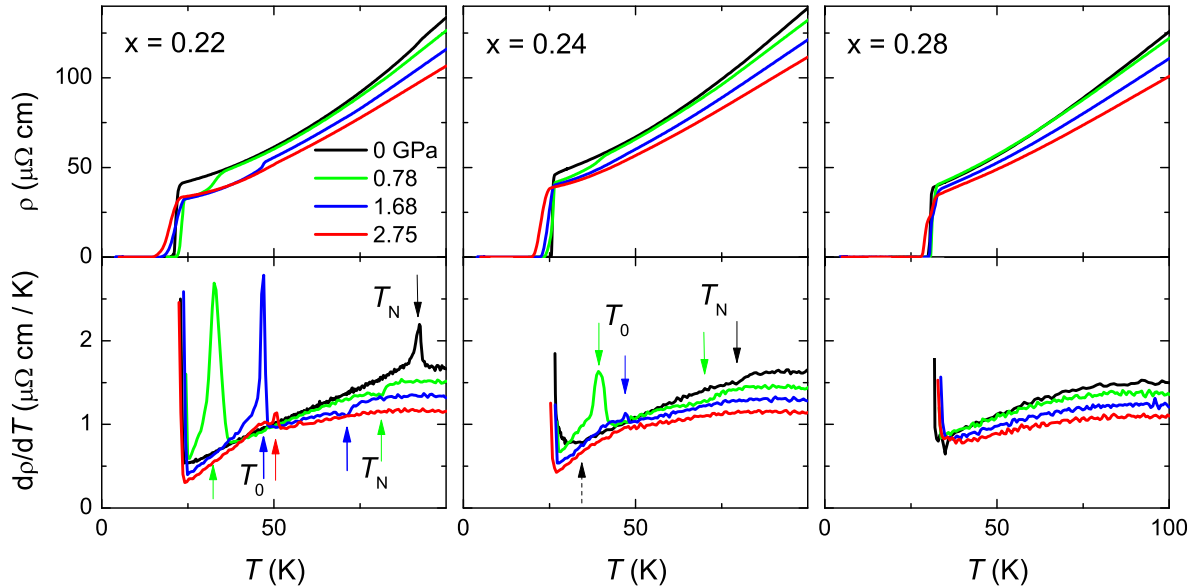


FIG. 1. Top: In-plane electrical resistivity of  $\text{Ba}_{1-x}\text{K}_x\text{Fe}_2\text{As}_2$  for  $x = 0.22, 0.24,$  and  $0.28$  (different columns) for four different pressures, as indicated. Bottom: Temperature derivative of the data in the top panels. The peak (dip) between 60 and 100 K signals the onset of stripelike antiferromagnetic order at  $T_N$  (arrows). The peak at lower temperature signals the onset of the tetragonal magnetic phase at  $T_0$  (arrows). In the lower middle panel ( $x = 0.24$ ), the dashed arrow marks the foot of the peak at  $T_0$  in the black curve at ambient pressure.

Ref. [3] and wavelength-dispersive x-ray spectroscopy [22], we obtain  $x = 0.22, 0.24,$  and  $0.28,$  respectively. These  $x$  values are also consistent with the measured antiferromagnetic ordering temperature  $T_N$  (which coincides with the structural transition from tetragonal to orthorhombic) [3], equal to  $91 \pm 2$  and  $79 \pm 5$  K, respectively for the two lower dopings. The sample with  $x = 0.28$  shows no magnetic or structural transition. The resistivity at room temperature of all samples lies between 250 and 350  $\mu\Omega$  cm, in agreement with previous studies [23]. As before [4], we have normalized the resistivity at  $T = 300$  K to 300  $\mu\Omega$  cm. Hydrostatic pressures up to 2.75 GPa were applied with a hybrid piston-cylinder cell [24], using a 50:50 mixture of *n*-pentane:isopentane. This pressure transmitting medium has been shown to present the best hydrostatic conditions, i.e., the smallest uniaxial pressure component, in the pressure range up to 3 GPa [25]. The pressure was measured via the superconducting transition of a lead wire inside the pressure cell. The electrical resistivity  $\rho$  was measured for a current in the basal plane of the orthorhombic crystal structure, with a standard four-point technique using a Lakeshore ac-resistance bridge. The transition temperatures are defined as follows:  $T_c$  is where  $\rho = 0$ ;  $T_N$  and  $T_0$  are detected as extrema in the derivative  $d\rho/dT$ .

### III. RESISTIVITY

Figure 1 shows the in-plane resistivity (top panels) and its temperature derivative (bottom panels) of each sample, for a selection of pressures.  $T_N$  is detected as a peak in the derivative for the first sample at ambient pressure, and then as a dip for higher pressures or doping. The transition at  $T_0$  shows up as a sharp peak, below  $T_N$ . For those concentrations

and applied pressures where both  $T_N$  and  $T_0$  are detected, the resistivity curves and their temperature derivatives resemble those of a sample with  $x = 0.25$  at ambient pressure, where the t-AF phase is present (see the Supplemental Material of Ref. [7].) In that publication, resistivity is identified as a good probe of  $T_0$  via a comparison with thermodynamic probes such as the thermal expansion or specific heat. In Fig. 2, the full set of derivative curves is displayed for  $x = 0.22$  and  $0.24$ , allowing one to track the anomalies at  $T_N$  and  $T_0$  as a function of pressure.

As previously reported for samples with lower doping [4],  $T_N$  decreases linearly with pressure. For  $x = 0.22$ , the peak in the derivative at  $T_N$  evolves into a dip at 0.48 GPa. We are able to follow this dip up to  $P = 2.0$  GPa, above which it disappears. The evolution of the peak at  $T_0$  is different. At 0.48 GPa, the peak at  $T_0$  appears.  $T_0$  goes up with pressure until it stays almost constant above 2.3 GPa. The height of the sharp peak at  $T_0$  increases slightly at first, and then decreases above  $P \simeq 1.5$  GPa. The behavior for  $x = 0.24$  is similar, but shifted to lower pressures.  $T_N$  can be followed only up to 0.94 GPa. The transition at  $T_0$  appears as a peak as soon as we apply pressure. In fact, a slight upturn of the derivative with decreasing  $T$ , indicative of an onset of the transition at  $T_0$ , can be seen even at ambient pressure. The onset is marked by an up-pointing dashed arrow in the lower middle panel of Fig. 1. We see that the new phase is present in this sample at  $P = 0$ . This provides a direct link between what was initially called the “new phase” and what is now known to be the t-AF phase. (In our previous study, a similar situation was found for  $x = 0.19$  at  $P = 1.08$  GPa. At zero magnetic field, a slight onset of the transition at  $T_0$  was seen above  $T_c$ , which was completely uncovered by a magnetic field of  $H = 15$  T shifting the  $T_c$  far below  $T_0$ , which is itself unaffected by the field [4].) This

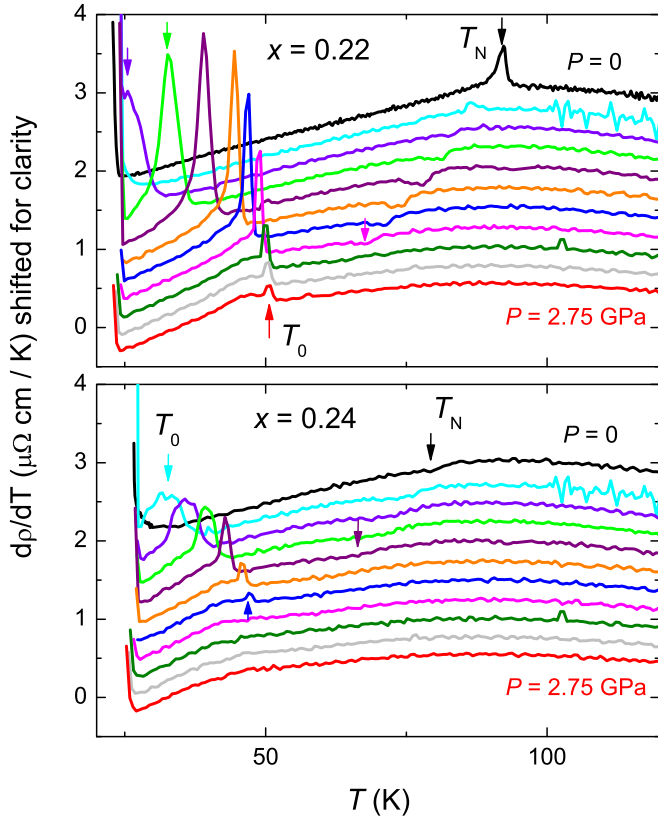


FIG. 2. Top: Temperature derivative of the resistivity of  $\text{Ba}_{1-x}\text{K}_x\text{Fe}_2\text{As}_2$  with  $x = 0.22$ , for 11 different pressures, from ambient pressure ( $P = 0$ ) at the top (black) to  $P = 2.75$  GPa at the bottom (red), with the following intermediate values:  $P = 0.28, 0.48, 0.78, 0.94, 1.37, 1.68, 2.0, 2.31,$  and  $2.4$  GPa. The curves are shifted for clarity. The black down-pointing arrow marks  $T_N$  at  $P = 0$ . The next down-pointing arrow marks  $T_N$  at the highest pressure where it can still be detected.  $T_0$  shows up as a peak at low temperature (e.g. down-pointing arrows below 50 K). The up-pointing arrow marks  $T_0$  at the highest pressure where the peak can still be detected. Bottom: The same for  $x = 0.24$ .

$x = 0.24$  sample is apparently right at the border of the t-AF phase, as a very tiny amount of either pressure or additional K content is enough to clearly induce the t-AF phase. The peak at  $T_0$  stays sharp but its height decreases above  $P \simeq 1$  GPa, and the last pressure where it is observed is 1.68 GPa. The curve at this pressure looks very much as the one at the highest pressure in the  $x = 0.22$  sample.

#### IV. TEMPERATURE-PRESSURE PHASE DIAGRAM

Figure 3 presents the temperature-pressure phase diagram for the three samples.  $T_N$  decreases linearly with  $P$ , with a slightly steeper slope at  $x = 0.24$ . By contrast,  $T_0$  rises rapidly, at least initially. At  $x = 0.22$ ,  $T_0$  saturates above  $P = 2.3$  GPa. At  $x = 0.24$ , we can no longer detect  $T_0$  above  $P = 1.68$  GPa (Fig. 2), the pressure at which it merges with the  $T_0$  line at  $x = 0.22$  (Fig. 3).

At  $x = 0.24$ , the phase diagram is such that if the  $T_0$  line (blue) saturates at high pressure, as it does in the case of  $x = 0.22$  (red  $T_0$  line), then a linear extension of the  $T_N$  line

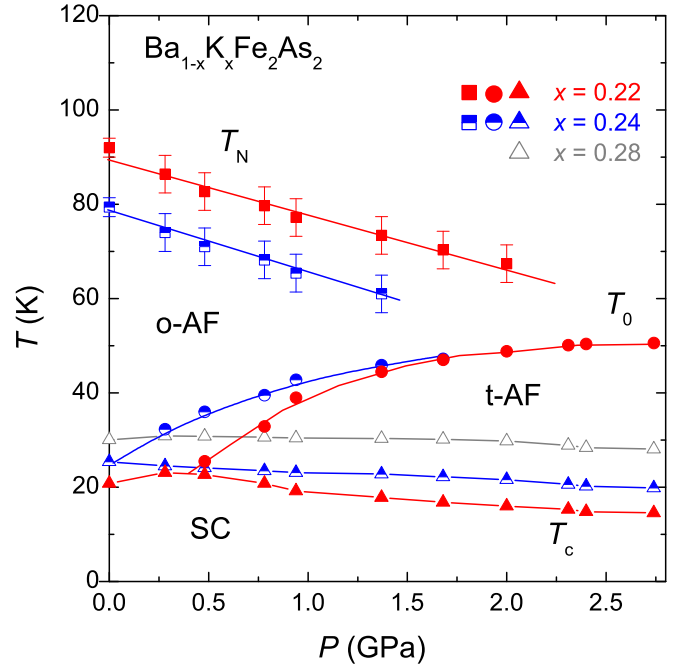


FIG. 3. Temperature-pressure phase diagram of  $\text{Ba}_{1-x}\text{K}_x\text{Fe}_2\text{As}_2$ , for  $x = 0.22, 0.24,$  and  $0.28$  (solid, half-solid, and open symbols, respectively), showing the orthorhombic antiferromagnetic (o-AF) transition temperature  $T_N$  (squares), the superconducting (SC) transition temperature  $T_c$  (triangles), and the tetragonal antiferromagnetic (t-AF) transition temperature  $T_0$  (circles).

(blue) will hit that  $T_0$  line, implying that the t-AF phase would persist to pressures beyond the end of the o-AF phase.

As for superconductivity, note that  $T_c$  decreases as soon as the tetragonal phase appears (Fig. 3), as found in prior studies of  $\text{Ba}_{1-x}\text{K}_x\text{Fe}_2\text{As}_2$  [4,26] and  $\text{Ba}_{1-x}\text{Na}_x\text{Fe}_2\text{As}_2$  [26,27], in agreement with the negative  $dT_c/dP$  expected from the Ehrenfest relation applied to the thermodynamic data [7].

#### V. TEMPERATURE-CONCENTRATION PHASE DIAGRAM

Combining our present results with those of our previous study [4], we plot the temperature-concentration phase diagram of  $\text{Ba}_{1-x}\text{K}_x\text{Fe}_2\text{As}_2$  in Fig. 4. For comparison, we also reproduce the phase diagram at zero pressure reported in Ref. [7]; the agreement with our own ambient-pressure data is excellent. We see that the  $T_N$  line moves down with pressure, in parallel fashion. This suggests that the critical concentration  $x_N$  where  $T_N$  goes to zero shifts down with pressure.

On the backdrop of this shrinking o-AF phase, the tetragonal magnetic phase undergoes a major expansion with pressure (Fig. 4). While the t-AF phase occupies a small area below  $T_N$  at ambient pressure, its area grows by an order of magnitude at  $P = 2.4$  GPa. In other words, at high pressure the tetragonal phase becomes the dominant magnetic phase in the temperature-concentration phase diagram of  $\text{Ba}_{1-x}\text{K}_x\text{Fe}_2\text{As}_2$ . A recent study of thermal expansion and specific heat revealed a complex phase diagram in  $\text{Ba}_{1-x}\text{Na}_x\text{Fe}_2\text{As}_2$  with an expanded tetragonal phase [28]. There, in agreement with our results, chemical pressure might lead to the expansion of the

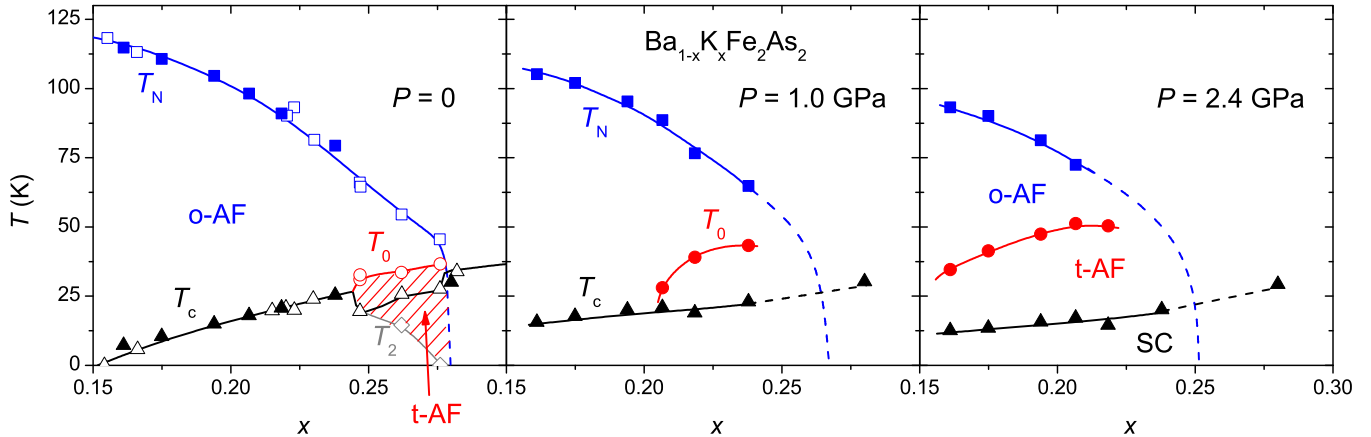


FIG. 4. Temperature-concentration phase diagram of  $\text{Ba}_{1-x}\text{K}_x\text{Fe}_2\text{As}_2$ , showing  $T_N$  (blue squares),  $T_0$  (red circles), and  $T_c$  (black triangles), for three different values of the applied pressure:  $P = 0$  (left panel), 1.0 GPa (middle panel), and 2.4 GPa (right panel). This includes data from our previous study [4]. Ambient-pressure data from Ref. [7] are also shown in the left panel (open symbols), including a transition back to the o-AF phase, below  $T_2$  (diamonds). All lines are a guide to the eye. The evolution from left to right, with increasing pressure, reveals a major expansion of the tetragonal magnetic phase (t-AF), on the backdrop of a shrinking stripe phase (o-AF). Extrapolating to higher pressure, we expect the former to become the dominant magnetic phase coexisting with superconductivity in  $\text{Ba}_{1-x}\text{K}_x\text{Fe}_2\text{As}_2$ .

tetragonal phase [28]. In the context of recent calculations, it may be that pressure favors the t-AF phase because it changes the ellipticity of the electron pockets in the Fermi surface of  $\text{Ba}_{1-x}\text{K}_x\text{Fe}_2\text{As}_2$  [16].

## VI. SUMMARY

In summary, we have shown that the new phase discovered in  $\text{Ba}_{1-x}\text{K}_x\text{Fe}_2\text{As}_2$  from sharp signatures in the resistivity under pressure [4] is the tetragonal antiferromagnetic phase observed and identified subsequently by various probes in both  $\text{Ba}_{1-x}\text{Na}_x\text{Fe}_2\text{As}_2$  [5,6] and  $\text{Ba}_{1-x}\text{K}_x\text{Fe}_2\text{As}_2$  [7–9]. Under pressure, this t-AF phase expands enormously, by an order of magnitude for 2.4 GPa in terms of the area it occupies in the temperature-concentration phase diagram, relative to the orthorhombic stripelike AF phase that dominates at ambient pressure. As a result, at high pressure, superconductivity exists on the border of a dominant tetragonal magnetic phase. It is then likely that fluctuations of that double- $Q$  phase play

a role in the pairing. Recent calculations suggest that such fluctuations could actually enhance  $T_c$  [19].

## ACKNOWLEDGMENTS

We thank A. V. Chubukov, R. M. Fernandes, S. A. Kivelson, C. Meingast, and J. Schmalian for fruitful discussions and J. Corbin for his assistance with the experiments. The work at Sherbrooke was supported by a Canada Research Chair, the Canadian Institute for Advanced Research, the National Science and Engineering Research Council of Canada, the Fonds de Recherche du Québec–Nature et Technologies, and the Canada Foundation for Innovation. Work in Ames was supported by the U.S. DOE, Office of Science, Basic Energy Sciences, Materials Science and Engineering Division. Ames Laboratory is operated for the U.S. DOE by Iowa State University under contract DE-AC02-07CH11358. The work in China was supported by the National Science Foundation of China and the Ministry of Science and Technology of China (No. 2011CBA00100).

- 
- [1] P. C. Canfield and S. L. Budk'ov, *Annu. Rev. Condens. Matter Phys.* **1**, 27 (2010).
- [2] D. K. Pratt, W. Tian, A. Kreyssig, J. L. Zarestky, S. Nandi, N. Ni, S. L. Bud'ako, P. C. Canfield, A. I. Goldman, and R. J. McQueeney, *Phys. Rev. Lett.* **103**, 087001 (2009).
- [3] S. Avci, O. Chmaissem, D. Y. Chung, S. Rosenkranz, E. A. Goremychkin, J. P. Castellán, I. S. Todorov, J. A. Schlueter, H. Claus, A. Daoud-Aladine, D. D. Khalyavin, M. G. Kanatzidis, and R. Osborn, *Phys. Rev. B* **85**, 184507 (2012).
- [4] E. Hassinger, G. Gredat, F. Valade, S. R. de Cotret, A. Juneau-Fecteau, J.-Ph. Reid, H. Kim, M. A. Tanatar, R. Prozorov, B. Shen, H.-H. Wen, N. Doiron-Leyraud, and L. Taillefer, *Phys. Rev. B* **86**, 140502(R) (2012).
- [5] S. Avci, O. Chmaissem, J. M. Allred, S. Rosenkranz, I. Eremin, A. V. Chubukov, D. E. Bugaris, D. Y. Chung, M. G. Kanatzidis, J.-P. Castellán, J. A. Schlueter, H. Claus, D. D. Khalyavin, P. Manuel, A. Daoud-Aladine, and R. Osborn, *Nat. Commun.* **5**, 3845 (2014).
- [6] F. Waßer, A. Schneidewind, Y. Sidis, S. Wurmehl, S. Aswartham, B. Büchner, and M. Braden, *Phys. Rev. B* **91**, 060505(R) (2015).
- [7] A. E. Böhmer, F. Hardy, L. Wang, T. Wolf, P. Schweiss, and C. Meingast, *Nat. Commun.* **6**, 7911 (2015).
- [8] B. P. P. Mallett, P. Marsik, M. Yazdi-Rizi, Th. Wolf, A. E. Böhmer, F. Hardy, C. Meingast, D. Munzar, and C. Bernhard, *Phys. Rev. Lett.* **115**, 027003 (2015).

- [9] J. M. Allred, S. Avci, D. Y. Chung, H. Claus, D. D. Khalyavin, P. Manuel, K. M. Taddei, M. G. Kanatzidis, S. Rosenkranz, R. Osborn, and O. Chmaissem, *Phys. Rev. B* **92**, 094515 (2015).
- [10] Y. Zheng, P. M. Tam, J. Hou, A. E. Böhrer, T. Wolf, C. Meingast, and R. Lortz, *Phys. Rev. B* **93**, 104516 (2016).
- [11] J. Lorenzana, G. Seibold, C. Ortix, and M. Grilli, *Phys. Rev. Lett.* **101**, 186402 (2008).
- [12] I. Eremin and A. V. Chubukov, *Phys. Rev. B* **81**, 024511 (2010).
- [13] E. Berg, S. A. Kivelson, and D. J. Scalapino, *Phys. Rev. B* **81**, 172504 (2010).
- [14] G. Giovannetti, C. Ortix, M. Marsman, M. Capone, J. van den Brink, and J. Lorenzana, *Nat. Commun.* **2**, 398 (2011).
- [15] P. M. R. Brydon, J. Schmiedt, and C. Timm, *Phys. Rev. B* **84**, 214510 (2011).
- [16] J. Kang, X. Wang, A. V. Chubukov, and R. M. Fernandes, *Phys. Rev. B* **91**, 121104(R) (2015).
- [17] X. Wang, J. Kang, and R. M. Fernandes, *Phys. Rev. B* **91**, 024401 (2015).
- [18] M. N. Gastiasoro and B. M. Andersen, *Phys. Rev. B* **92**, 140506 (2015).
- [19] R. M. Fernandes, S. A. Kivelson, and E. Berg, *Phys. Rev. B* **93**, 014511 (2016).
- [20] J. M. Allred, K. M. Taddei, D. E. Bugaris, M. J. Krogstad, S. H. Lapidus, D. Y. Chung, H. Claus, M. G. Kanatzidis, D. E. Brown, J. Kang, R. M. Fernandes, I. Eremin, S. Rosenkranz, O. Chmaissem, and R. Osborn, [arXiv:1505.06175](https://arxiv.org/abs/1505.06175).
- [21] H. Luo, Z. Wang, H. Yang, P. Cheng, X. Zhu, and H.-H. Wen, *Supercond. Sci. Technol.* **21**, 125014 (2008).
- [22] M. A. Tanatar, W. E. Straszheim, H. Kim, J. Murphy, N. Spyrisson, E. C. Blomberg, K. Cho, J.-Ph. Reid, B. Shen, L. Taillefer, H.-H. Wen, and R. Prozorov, *Phys. Rev. B* **89**, 144514 (2014).
- [23] Y. Liu, M. A. Tanatar, W. E. Straszheim, B. Jensen, K. W. Dennis, R. W. McCallum, V. G. Kogan, R. Prozorov, and T. A. Lograsso, *Phys. Rev. B* **89**, 134504 (2014).
- [24] I. R. Walker, *Rev. Sci. Instrum.* **70**, 3402 (1999).
- [25] W. J. Duncan, O. P. Welzel, C. Harrison, X. F. Wang, X. H. Chen, F. M. Grosche, and P. G. Niklowitz, *J. Phys.: Condens. Matter* **22**, 052201 (2010).
- [26] S. L. Bud'ko, M. Sturza, D. Y. Chung, M. G. Kanatzidis, and P. C. Canfield, *Phys. Rev. B* **87**, 100509(R) (2013).
- [27] S. L. Bud'ko, D. Y. Chung, D. Bugaris, H. Claus, M. G. Kanatzidis, and P. C. Canfield, *Phys. Rev. B* **89**, 014510 (2014).
- [28] L. Wang, F. Hardy, A. Böhrer, T. Wolf, P. Schweiss, and C. Meingast, *Phys. Rev. B* **93**, 014514 (2016).